momentum of an emitted phonon is limited by the spatial extent of the localized exciton state. Because the energy of an acoustic phonon is determined by its momentum, an exciton relaxation bottleneck occurs when the exciton cannot emit a single phonon with enough energy to relax to the next level. Instead, the excitons must relax via higher ordered processes such as a multiphonon emission. The relaxation bottleneck has been controversial; it has to our knowledge never been directly observed, but it would be important as it could prevent the practical use of certain low-dimensional structures.

In Fig. 4 (20 K), there are several places along the wire that show unusually low-energy PL. In particular, Fig. 5 magnifies the set of states from position 27.5 μm of Fig. 4. Those states appear at precisely the same position to within our spatial resolution and are especially isolated from other states. The intensity of the PL peak at 1,565.5 meV increases substantially at lower temperatures, while the intensity of the lower energy peak at 1,563.6 meV actually decreases. The excitons apparently radiate from higher energy states before relaxing to the lowest available quantum dot state. This result could be interpreted in two ways. One possibility is that these are a set of isolated quantum dots, but so closely spaced that we cannot spatially separate them, in which case thermally activated excitons may hop between quantum dots. As the temperature is lowered, the excitons are unable to hop into the lowest states. However, given that the luminescent quantum dots are quite sparse along the wire and the island growth model implies that wide regions of the wire should be anticorrelated, such a series of closely spaced, isolated quantum dots is implausible. We prefer to interpret the series of states as excited states of a single quantum dot. The exciton relaxation bottleneck accounts for our observation that the lowest energy states are unoccupied. It is not obvious why the bottleneck vanishes at high temperatures, but multiphonon processes including emission and absorption are temperature-dependent. In this example the effect disappears above 15 K which corresponds to an acoustic phonon occupation up to 1.2 meV, comparable to the observed energy spacing between these states. This is a clear observation of a relaxation bottleneck in quantum dots. Although we have found other instances of this effect in our wire PL, Fig. 5 is the cleanest example that we have observed.

As previously mentioned, multiple quantum wires at T-intersections have been formed into an optically pumped laser[4]. Our quantum wire sample is nominally identical to one of the 22 matched quantum wires used in that laser. The laser in that report was operated at 2 K, at which according to our present measurements the individual quantum wires may have been dominated by quantum dot states at low exciton densities. It is an open question as to how or whether the quantum dot states reported here contribute to the lasing at high exciton densities. □

Received 21 May; accepted 18 August 1997.

1. Loudon, R. One-dimensional hydrogen atom. *Am. J. Phys.* **27,** 649–655 (1959).
2. Chang, Y.-C., Chang, L. L. & Esaki, L. A new one-dimensional quantum well structure. *Appl. Phys. Lett.* **47,** 1324–1326 (1985).
3. Pfeiffer, L. N. *et al.* Formation of a high quality two-dimensional electron gas on cleaved GaAs. *Appl. Phys. Lett.* **56,** 1697–1699 (1990).
4. Wegscheider, W. *et al.* Lasing from excitons in quautum wires. *Phys. Rev. Lett.* **71,** 4071–4074 (1993).
5. Wegscheider, W., Pfeiffer, L. N., West, K. W. & Leibenguth, R. E. Current injection GaAs/AlGaAs quantum wire lasers fabricated by cleaved edge overgrowth. *Appl. Phys. Lett.* **65,** 2510–2512 (1994).
6. Goñi, A. R. *et al.* Observation of quantum wire formation at intersecting quantum wells. *Appl. Phys. Lett.* **61,** 1956–1958 (1992).
7. Someya, T., Akiyama, H. & Sakaki, H. Tightly confined one-dimensional states in T-shaped GaAs edge quantum wires with AlAs barriers. *Appl. Phys. Lett.* **66,** 3672–3673 (1995).
8. Hasen, J. *et al.* Large excitonic confinement in asymmetric quantum T wires. *Superlattices and Microsctructures* (in the press).
9. Gislason, H., Langbein, W. & Hvam, J. M. Asymmetric GaAs/AlGaAs T wires with large confinement energies. *Appl. Phys. Lett.* **69,** 3248–3250 (1996).
10. Hess, H. F., Betzig, E., Harris, T. D., Pfeiffer, L. N. & West, K. W. Near-field spectroscopy of the quantum constituents of a luminescent system. *Science* **264,** 1740–1745 (1994).
11. Zrenner, A. *et al.* Quantum dots formed by interface fluctuations in AlAs/GaAs coupled quantum well structures. *Phys. Rev. Lett.* **72,** 3382–3385 (1994).
12. Brunner, K., Abstreiter, G., Böhm, G., Tränkle, G. & Weimann, G. Sharp-line photoluminescence of excitons localized at GaAs/AlGaAs quantum well inhomogeneities. *Appl. Phys. Lett.* **64,** 3320–3322 (1994).
13. Gammon, D., Snow, E. S., Shanabrook, B. V., Katzer, D. S. & Park, D. Fine structure splitting in the optical spectra of single GaAs quantum dots. *Phys. Rev. Lett.* **76,** 3005–3008 (1996).
14. Benisty, H., Sotomayor-Torrès, C. M. & Weisbuch, C. Intrinsic mechanism for the poor luminescence properties of quantum-box systems. *Phys. Rev. B* **44,** 10945–10948 (1991).

Acknowledgements. We thank H. U. Baranger, T. D. Harris, P. B. Littlewood and R. Zimmermann for discussions.

Correspondence and requests for materials should be addressed to J.H. (e-mail: joel@lucent.com).

Large magnetoresistance in non-magnetic silver chalcogenides

R. Xu*†, A. Husmann*, T. F. Rosenbaum*, M.-L. Saboungi†, J. E. Enderby† & P. B. Littlewood‡

* *The James Franck Institute and Department of Physics, The University of Chicago, Chicago, Illinois 60637, USA*
† *Materials Science Division, Argonne National Laboratory, Argonne, Illinois 60439, USA*
‡ *Bell Laboratories, Lucent Technologies, Murray Hill, New Jersey 07974, USA*

Several materials have been identified over the past few years as promising candidates for the development of new generations of magnetoresistive devices. These range from artificially engineered magnetic multilayers[1] and granular alloys[2,3], in which the magnetic-field response of interfacial spins modulates electron transport to give rise to 'giant' magnetoresistance[4], to the manganite perovskites[5–7], in which metal–insulator transitions driven by a magnetic field give rise to a 'colossal' magnetoresistive response (albeit at very high fields). Here we describe a hitherto unexplored class of magnetoresistive compounds, the silver chalcogenides. At high temperatures, the compounds Ag_2S, Ag_2Se and Ag_2Te are superionic conductors; below ~400 K, ion migration is effectively frozen and the compounds are non-magnetic semiconductors[8,9] that exhibit no appreciable magnetoresistance[10]. We show that slightly altering the stoichiometry can lead to a marked increase in the magnetic response. At room temperature and in a magnetic field of ~55 kOe, $Ag_{2+\delta}Se$ and $Ag_{2+\delta}Te$ show resistance increases of up to 200%, which are comparable with the colossal-magnetoresistance materials. Moreover, the resistance of our most responsive samples exhibits an unusual linear dependence on magnetic field, indicating both a potentially useful response down to fields of practical importance and a peculiarly long length scale associated with the underlying mechanism.

Although substantial values of magnetoresistance are found for a variety of materials at low temperatures and in high magnetic fields, useful devices must operate at room temperature and in modest fields, $H < 1$ kOe. For non-magnetic metals, semimetals and semiconductors, the normalized magnetoresistance, $\Delta\rho(T,H)/\rho(T,0)$, is usually negligible for such fields at $T \sim 300$ K (ref. 11). Narrow-gap semiconductors such as PbTe (ref. 12) and InSb (ref. 13) do indeed have a formidable low-field magnetoresistance at room temperature (0.01–1% for $H = 1$ kOe), but the characteristic resistivities are so large that the intrinsic device noise becomes the limiting factor. Balancing these constraints has led to permalloy ($Ni_{0.81}Fe_{0.19}$), with a saturation value $\Delta\rho/\rho \sim 2.5\%$ at $H \sim 5$ Oe, becoming the material of choice for standard applications[14]. Giant-magnetoresistance compounds seem to hold the greatest promise as replacement materials in the short term, with $\Delta\rho/\rho$ as high as 40% for $H \leqslant 1$ kOe being observed in Cu/Co multilayers at room temperature[15]. Both the high field scale and the resistivity ($\sim 10^4$ μΩ cm, comparable in magnitude with narrow-gap semiconductors) are present obstacles for potential colossal-magnetoresistance devices.

Silver selenide and silver telluride are narrow-gap self-doped degenerate n-type semiconductors. In their high-temperature (α) phase, electrical transport proceeds via a well-orchestrated coupling of microscopic lattice distortions to the ion migration dynamics. The structural transformation into the β-phase opens an energy gap as small as a few hundredths of an electronvolt. The electron density in the conduction band is determined largely by the stoichiometric index, δ. We cut specimens with typical dimensions 1–3 mm on a side and 1 mm thick from long boules with a designated purity of 99.999%. Slight gradients in stoichiometry along the length of the boule permitted the choice of samples with a range of electron densities. For both semiconductors, the nominal δ is approximately 0.01, with $\rho(300\,\mathrm{K}) \leqslant 10^3\ \mu\Omega\,\mathrm{cm}$. We performed four-probe resistivity and five-probe Hall coefficient measurements in fields up to 55 kOe using a conventional a.c. bridge technique in the ohmic and frequency-independent limits. The relative error in the magnetoresistivity is less than 0.01%; there is an absolute uncertainty, however, of 25% because of the finite extent of the silver epoxy contacts on millimetre-scale samples. We applied hydrostatic pressure with a BeCu piston–anvil self-locking pressure clamp, using silicone oil as the pressure medium and a chip of $(V_{0.99}Ti_{0.01})_2O_3$ as the manometer[16].

We plot in Fig. 1 an overview of the temperature dependence of the resistivity of $Ag_{2+\delta}Se$ and $Ag_{2+\delta}Te$ for a series of applied magnetic fields. The field is applied perpendicular to the current direction; measurements of the longitudinal magnetoresistance also show a considerable effect, but at least a factor of 2 smaller than the transverse magnetoresistance. The temperature dependence of $\rho(H = 0)$ is consistent with impurity band electrons on the delocalized side of the Mott metal–insulator transition[17]. Between $T = 4.2$ K and $T = 60$ K for $Ag_{2+\delta}Se$ (100 K for $Ag_{2+\delta}Te$), the resistivity rises because n is constant and the phonon scattering increases with T. At higher T, n becomes activated and ρ decreases with increasing T in accordance with the usual behaviour of small-gap semiconductors.

The large size and the magnetic-field dependence of the normalized magnetoresistance can seen explicitly in Fig. 2. There is no evidence of saturation up to at least 55 kOe over the entire temperature range. $\Delta\rho/\rho$ increases linearly with increasing H at high T, with a tendency towards a slightly sublinear dependence above tens of kOe at low T. The normal solution of the Boltzmann equation for magnetoresistance yields a dependence on H^2, although scattering off the lattice and/or spin fluctuations can produce $\Delta\rho/\rho \propto H$. As can be seen in the inset to Fig. 2, the magnetoresistance falls below 1% by $H = 100$ Oe. The surprise in our data is that the pertinent field scale at which the magnetoresistance crosses over from a quadratic to a linear dependence on H is so small: $H_c \approx 10$ Oe, with the exact value being dependent on the range of fit. It is difficult to identify a physical length scale that corresponds to this magnetic field value. Yet the value of H_c seems to be related intimately to the large magnetoresistive response. Samples that exhibit a smaller magnetoresistance also display a larger crossover field, up to two orders of magnitude higher.

We compare in Fig. 3 the high-field (40 kOe), normalized magnetoresistance near room temperature for $Ag_{2+\delta}Se$, $Ag_{2+\delta}Te$, and a representative colossal-magnetoresistance compound, $La_{0.75}Ca_{0.25}MnO_3$ (ref. 18). The absolute value of the magnetoresistance is pronounced for all three, but of opposite sign—positive for the silver chalcogenides and negative for the manganite perovskites—reflecting completely different physical mechanisms. This difference is also exemplified in the contrasting temperature evolution of the magnetoresistance. $\Delta\rho/\rho$ of the colossal-magnetoresistance material changes rapidly in a narrow temperature range and must either be fine-tuned so that the metal–insulator transition temperature is near 300 K or be modulated via interfacial tunnelling in fine-grained polycrystals[19]. In contrast, the silver chalcogenide data evolve smoothly with temperature and exhibit no sharp features.

The question remains of how to optimize the normalized magnetoresistance for $Ag_{2+\delta}Se$ and $Ag_{2+\delta}Te$. As demonstrated in Fig. 4, it seems that the carrier density is a key variable. Analysis of the linear Hall response at $H = 5$ kOe in the single carrier 'exhaustion' regime (temperatures below the maximum of $\rho(T)$ in Fig. 1, where the Hall coefficient, R_H, becomes temperature-independent), shows an increasing magnetoresistance with decreasing R_H (increasing n). An increase in the intrinsic carrier density from 2.5×10^{17} to $9 \times 10^{17}\,\mathrm{cm}^{-3}$ results in an increase in $\Delta\rho(T = 4.5\,\mathrm{K}, H = 55\,\mathrm{kOe})/\rho(T = 4.5\,\mathrm{K}, H = 0)$ from 200% to 350%. Moreover, identically doped samples of $Ag_{2+\delta}Se$ and $Ag_{2+\delta}Te$ have identically large magnetoresistances.

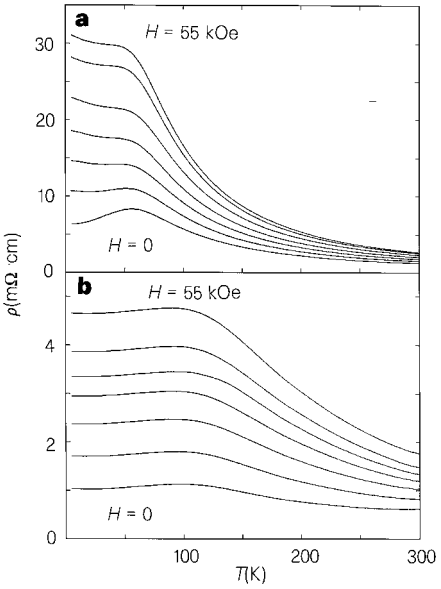

Figure 1 Resistivity ρ as a function of temperature T at a series of magnetic fields $H = 0$, 9, 17, 26, 36, 48 and 55 kOe for $Ag_{2+\delta}Se$ (**a**) and $H = 0$, 10, 20, 29, 35, 43 and 55 kOe for $Ag_{2+\delta}Te$ (**b**).

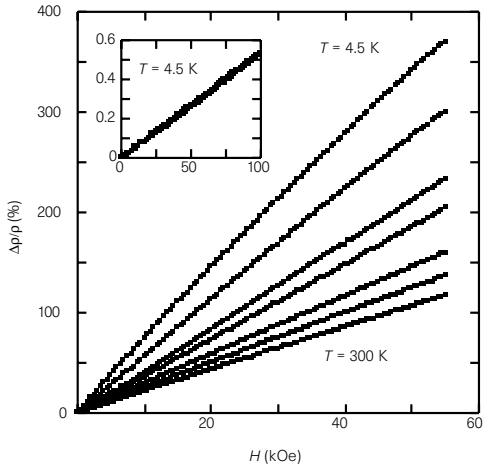

Figure 2 The normalized magnetoresistance $\Delta\rho(T, H)/\rho(T, 0)$ for $Ag_{2+\delta}Se$ as a function of magnetic field H at a series of temperatures $T = 4.5$, 30, 60, 90, 180, 270 and 300 K. Inset, the linear field dependence continues down to H values of a few Oe, implying a very large characteristic length scale.

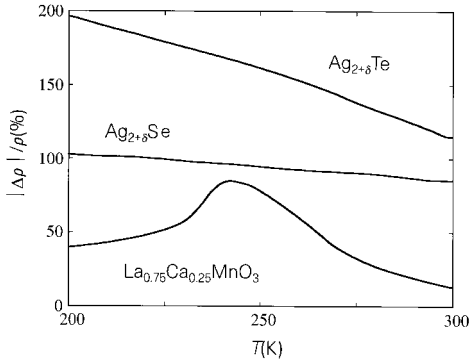

Figure 3 Comparison of the normalized magnetoresistance of the silver chalcogenides and a representative colossal-magnetoresistance material at $H = 40$ kOe.

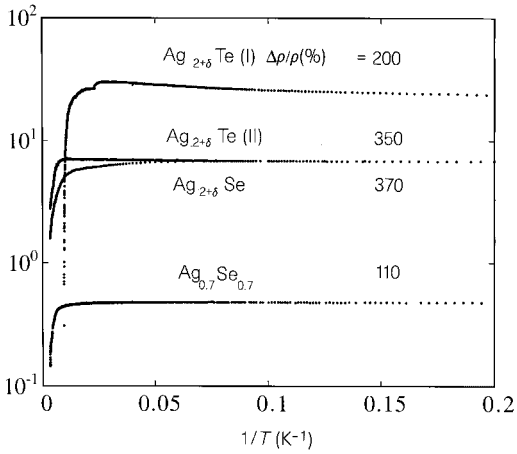

Figure 4 Hall coefficient R_H (n-type) plotted against T^{-1} for a set of silver chalcogenide samples labelled by their magnetoresistive response (at $T = 4.5$ K and $H = 55$ kOe). Carrier density in the intrinsic, low-temperature limit seems to be a key causal parameter.

The classical, orbital magnetoresistance is controlled by the ratio of the cyclotron frequency to the scattering rate, $\omega_c\tau = eH\tau/m^*c$. Doped narrow-gap semiconductors have small effective masses, $m^* \approx 0.02m_e$ ($0.08m_e$) for Ag_2Te (Ag_2Se) (ref. 20), which gives a large magnetoresistance. Furthermore, good metallic conduction can be obtained even at low carrier densities because the combination of a small m^* and a large dielectric constant pushes the metal–insulator transition boundary to low densities. One expects a positive magnetoresistance, quadratic at low fields, and saturating for $\omega_c\tau > 1$. A non-saturating, but still quadratic, magnetoresistance can occur with perfect compensation along with a vanishing Hall effect, as would be expected in the intrinsic regime at high T.

Despite the advantageous standing of narrow-gap semiconductors, the classical picture seems incapable of explaining the silver chalcogenide data, even allowing for a crossover from degenerate to non-degenerate transport seen in $\rho(T > 100\,\mathrm{K})$. The magnetoresistance is linear down to very low fields; it shows little sign of saturation at high fields, even though $\omega_c\tau > 5$ at the highest fields for the $Ag_{2+\delta}Te$ sample in Fig. 1; and it is only weakly temperature-dependent, with no evidence for a crossover associated with degenerate to non-degenerate carriers. Inhomogeneous density fluctuations, on a scale larger than the mean free path but much smaller than the sample size, can produce a magnetoresistance linear in H with $\Delta\rho/\rho \approx \omega_c\tau$ (ref. 21). The electronic and point defects that occur in the silver chalcogenides for $\delta \geqslant 10^{-4}$ (refs 22, 23) might provide a source of such density fluctuations, leading in principle to a high-field transverse magnetoresistance of the observed size. However, this mechanism cannot explain either the anomalously low H_c (at $\omega_c\tau \ll 1$) or the correlation between R_H and $\Delta\rho/\rho$ demonstrated in Fig. 4.

We have studied samples doped as far away from 2 : 1 stoichiometry as $Ag_{0.70}Se_{0.30}$, where $R_H(T \to 0)$ approaches $0.4\,\mathrm{cm^3\,C^{-1}}$ ($n > 10^{19}\,\mathrm{cm^{-3}}$) and $\rho(T = 300\,\mathrm{K}) = 350\,\mu\Omega\,\mathrm{cm}$ (Fig. 4). In this case, $\Delta\rho/\rho$ falls to 110%, implying an optimal value for δ between 0.01 and 0.33. A significant advantage of the silver chalcogenides is that the Ag stoichiometry could be controlled precisely in future experiments through electrochemical techniques because silver β-alumina is readily available. The results of applying hydrostatic pressure are also encouraging. A pressure of only 7 kbar halved the room-temperature resistivity of the $Ag_{2+\delta}Se$ sample of Fig. 2 without reducing the magnetoresistance. In contrast, the magnetoresistance in colossal-magnetoresistance compounds is severely suppressed by pressure[24]. Hence, the strategy of introducing internal pressure through chemical means or, alternatively, interfacial stress in a silver chalcogenide thin film, may help satisfy the device goal of a small ρ without sacrificing the large magnetoresistance. □

Methods

High-purity Ag_2Se and Ag_2Te (99.999% pure) were used as received from Johnson Matthey Corporation and United Mineral Corporation. The stoichiometric materials were ground and loaded into four outgassed fused silica ampoules inside a helium glovebox, and appropriate amounts of silver or selenium were added to reach the desired compositions. The selenium was treated to remove the oxide coatings by filtering through a fine-size frit near the melting point. The samples were sealed under vacuum, heated in a rocking furnace above their respective melting points for 24 h and left to cool in a horizontal position. Powder X-ray diffraction gave the expected orthorhombic structure at room temperature with a grain size of at least 500 nm. No additional phases were detected in any sample. SQUID magnetometry on $Ag_{2+\delta}Se$ showed no evidence for paramagnetic impurities with an essentially temperature-independent diamagnetic response, $\chi(T = 4.5\,\mathrm{K}) = -1.7 \times 10^{-7}\,\mathrm{cm^{-3}}$.

Received 9 May; accepted 27 August 1997.

1. Baibich, M. *et al.* Giant magnetoresistance of (001)Fe/(001)Cr magnetic superlattices. *Phys. Rev. Lett.* **61,** 2472–2475 (1988).
2. Berkowitz, A. E. *et al.* Giant magnetoresistance in heterogeneous Cu–Co alloys. *Phys. Rev. Lett.* **68,** 3745–3748 (1992).
3. Xiao, J. Q., Jiang, J. S. & Chien, C. L. Giant magnetoresistance in nonmultilayer magnetic systems. *Phys. Rev. Lett.* **68,** 3749–3752 (1992).
4. Camley, R. E. & Stamps, R. L. Magnetic multilayers: spin configurations, excitations and giant magnetoresistance. *J. Phys. Cond. Mater.* **5,** 3727–3786 (1993).
5. Searle, C. W. & Wang, S. T. Studies of the ionic ferromagnet (LaPb)MnO_3. III. Ferromagnetic resonance studies. *Can. J. Phys.* **47,** 2703–2708 (1969).
6. Jin, S. *et al.* Thousandfold change in resistivity in magnetoresistive La–Ca–Mn–O films. *Science* **264,** 413–415 (1994).
7. Tokura, Y. *et al.* Origins of colossal magnetoresistance in perovskite-type manganese oxides. *J. Appl. Phys.* **79,** 5288–5291 (1996).
8. Dalven, R. & Gill, R. Energy gap in β-Ag_2Se. *Phys. Rev.* **159,** 645–649 (1967).
9. Junod, P., Heidiger, H., Kilchör, B. & Wullschleger, J. Metal–non-metal transition in silver chalcogenides. *Phil. Mag.* **36,** 941–958 (1977).
10. Junod, P. Relations entre la structure cristalline et les propriétés électroniques des combinaisons Ag_2S, Ag_2Se, Cu_2Se. *Helv. Phys. Acta* **32,** 567–600 (1959).
11. Jan, J.-P. in *Solid State Physics*, Vol. 5 (eds Seitz, F. & Turnbull, D.) 1–96 (Academic, New York, 1957).
12. Allgaier, R. S., Restorff, J. B. & Houston, B. Weak- and strong-field magnetoresistance in (111)-oriented n-type PbTe epitaxial films between 1.8 and 300 K. *J. Appl. Phys.* **53,** 3110–3116 (1982).
13. Schönwald, H. Die Beweglichkeit der langsamen und schnellen Löcher in Indiumantimonid. *Z. Naturf.* **19a,** 1276–1296 (1964).
14. Brug, J. A., Anthony, T. C. & Nickel, J. H. Magnetic recording head materials. *Mater. Res. Soc. Bull.* **21,** 23–27 (1996).
15. Parkin, S. S. P., Li, Z. G. & Smith, D. J. Giant magnetoresistance in antiferromagnetic Co/Cu multilayers. *Appl. Phys. Lett.* **58,** 2710–2712 (1991).
16. Rosenbaum, T. F., Carter, S. A. & Honig, J. M. High sensitivity sensor for moderate pressures. *Rev. Sci. Instrum.* **67,** 617–618 (1996).
17. Mott, N. F. *The Metal–Insulator Transition* (Taylor and Francis, London, 1974).
18. Schiffer, P. *et al.* Low temperature magnetoresistance and the magnetic phase diagram of $La_{1-x}Ca_xMnO_3$. *Phys. Rev. Lett.* **75,** 3336–3339 (1995).

19. Hwang, H. *et al.* Spin-polarized intergrain tunneling in $La_{2/3}Sr_{1/3}MnO_3$. *Phys. Rev. Lett.* **77,** 2041–2044 (1996).
20. Aliev, S. A. & Aliev, F. F. Band parameters and energy structure of β-Ag_2Se. *Izv. Akad. Nauk SSSR, Neorgan. Mater.* **21,** 1869–1872 (1985).
21. Herring, C. Effect of random inhomogeneities on electrical and galvanomagnetic measurements. *J. Appl. Phys.* **31,** 1939–1953 (1960).
22. v. Oehsen, U. & Schmalzried, H. Thermodynamic investigations of Ag_2Se. *Ber. Bunsenges. Phys. Chem.* **85,** 7–14 (1981).
23. Valverde, N. Coulometrische Titrationen zur Bestimmung des Homogenitätsbereiches von festem Silbersulfid, Silberselenid und Silbertellurid. *Z. Phys. Chem. NF* **70,** 113–127 (1970).
24. Khazeni, K. *et al.* Effect of pressure on the magnetoresistance of single crystal $Nd_{0.5}Sr_{0.36}Pb_{0.14}MnO_{3-\delta}$. *Phys. Rev. Lett.* **76,** 295–298 (1996).

Acknowledgements. We thank D. L. Price and B. J. Wuensch for discussions. The work at the University of Chicago was supported primarily by the MRSEC Program of the National Science Foundation. The work at Argonne National Laboratory was supported by DOE Basic Energy Sciences.

Correspondence and requests for materials should be addressed to T.F.R. (e-mail: t-rosenbaum@uchicago.edu).

NMR evidence for excess non-bridging oxygen in an aluminosilicate glass

Jonathan F. Stebbins* & Zhi Xu†

** Department of Geological and Environmental Sciences, and*
† Department of Materials Science and Engineering, Stanford University, Stanford, California 94305-2115, USA

The most common of man-made glasses have aluminosilicate compositions, and such glasses also form from rapidly cooling magmas[1]. Oxygen is the most abundant element in these materials, where it occupies either 'bridging' (BO) or 'non-bridging' (NBO) sites. BOs link two AlO_4 or SiO_4 tetrahedra, thereby providing strong, long-lived bonds between the smallest structural units of the aluminosilicate network. NBOs provide a relatively weak connection between one tetrahedral cation (Al or Si) and one or more network modifier cations—such as Ca^{2+} or Na^+—that are not an integral part of the tetrahedral network. The relative abundance of these weakly bonded NBOs is critical in determining the thermodynamic and dynamical properties of aluminosilicate glasses and melts[1–3]. For glasses of 'tectosilicate' composition, where the charge of the modifier cation equals the number of aluminium atoms (as in $NaAlSi_3O_8$ or $CaAl_2Si_2O_8$), the conventional view of glass structure is that only BOs are present[1,4]. Here we present experimental observations that contradict this view. Our NMR measurements of $CaAl_2Si_2O_8$, which determine directly the relative abundances of BO and NBO, indicate that a considerable amount of NBO can be present in a tectosilicate glass. These excess NBOs will increase the entropy and heat capacity of the corresponding liquid and decrease its viscosity, as well as modifying flow and diffusion mechanisms[2,3]. As the most common rhyolitic magmas and the molten precursors of glass ceramics have near-tectosilicate compositions[1,4], our results require a reassessment of the high-temperature liquid properties that control many processes in the Earth and in industry.

The viscosity of a binary silicate liquid (such as $CaSiO_3$ or Na_2SiO_3) increases progressively as the network modifier oxide (CaO or Na_2O) is replaced by Al_2O_3. At a point near the 1 : 1 ratio of CaO and Al_2O_3 (or Na_2O and Al_2O_3), the viscosity reaches a maximum[5]. According to the conventional model of aluminosilicate structure[1,4], this viscosity increase arises from a gradual conversion of NBO to BO. This follows from requiring that all of the Al remain in AlO_4 tetrahedra, each oxygen atom of which is bonded to no more than one other tetrahedral cation. Because this replacement results in the substitution of relatively weak bonds between modifier cations and NBO by stronger, long-lived bonds between BO and tetrahedral cations, the viscosity increases. Furthermore, with increasing Al_2O_3 content, fewer modifier cations are available to attack and weaken the strong BO bonds, thereby further contributing to the increase in viscosity. This general picture provides a good qualitative explanation for the behaviour of complex natural systems, such as the enormous difference in viscosity—and thus eruptive style—between basaltic and rhyolitic magmas. Basalts have relatively low silica contents, on average about 1 NBO per tetrahedral cation (T), and usually erupt as quiescent flows, whereas rhyolites have much higher silica contents, NBO/T close to 0, and often erupt as viscous domes or in catastrophic explosions.

At a 1 : 1 ratio of the charge of the modifier cation to the number of aluminium atoms, the liquid has the stoichiometry of tectosilicates such as feldspars and quartz. Such liquids and glasses are often described as having a 'fully polymerized' structure—a somewhat randomized version of the corresponding crystal structure, with no NBO. The microscopic confirmation of this assumption is limited, in spite of the fact that it is the basis for a number of models describing the viscosity[6] and thermodynamics[7] of aluminosilicates. X-ray scattering data on feldspar-composition glasses are consistent with disordered framework structures[8] as expected for the 'fully polymerized' liquids and glasses, but minor amounts of other non-framework species, such as NBO or AlO_5, generally cannot be detected. In Raman[1,9] and ^{29}Si MAS NMR spectra[10,11], peaks for tetrahedral units with NBO overlap those containing only BO, making it also difficult to detect variations from the conventional approximation.

Precise measurements of the viscosity of Na- and Ca-aluminosilicate liquids have demonstrated that the viscosity maxima actually occur at a higher Al_2O_3 content than the ideal 1 : 1 ratio, suggesting that there is a considerable concentration of NBO even at the tectosilicate composition[12,13]. Displaced viscosity maxima in Ca-aluminosilicates were also suggested by less accurate, earlier data[6]. Oxygen-17 NMR is an ideal method by which to investigate directly whether NBO is indeed present at the 1 : 1 ratio[14,15]. Figure 1 shows ^{17}O magic-angle-spinning (MAS) NMR spectra of two glass samples

Table 1 Composition (in mol%) of glass samples similar to $CaAl_2Si_2O_8$

	Glass A	Glass B
SiO_2	49.6 ± 0.1	49.4
Al_2O_3	25.0 ± 0.2	25.2
CaO	25.5 ± 0.1	25.3
NBO predicted	0.5 ± 0.2	0.1
NBO observed	5 ± 1	4

Glass A was made by melting dried CaO, Al_2O_3 and 45% ^{17}O SiO_2 at 1,610 °C in a sealed platinum tube, and was analysed by electron microprobe. Uncertainties in composition are 2σ estimates from 4 to 8 repeated analyses. Glass B was made from glass A by adding 0.50 wt% Al_2O_3 and remelting. Both glasses contain about 0.07 mol% CoO, added to reduce spin-lattice relaxation time. NBO content (% of total oxygen) is predicted from the excess of (CaO + CoO) over Al_2O_3. The observed NBO content was derived from the 1D MAS NMR spectra assuming a symmetric peak shape, as is commonly observed in binary silicate glass compositions[15,16].

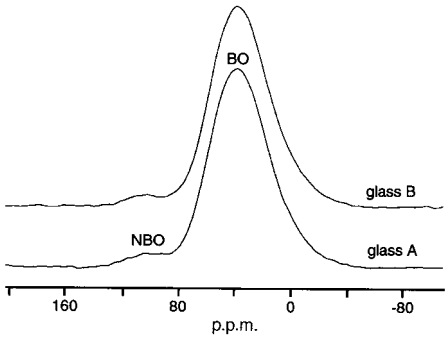

Figure 1 Oxygen-17 MAS NMR spectra of glasses A and B. The spectra were referenced to H_2O and collected at 54.2 MHz with a spinning rate of 12 kHz. Single 0.3-μs pulses (with roughly 10° radiofrequency tip angle for solid) were used, with a delay of 1 s. No differential relaxation was observed.